Chapter 1

GRAVITATIONAL LENSING; FROM μ-LENSING TO COSMIC SHEAR EXPERIMENTS

Francis Bernardeau

Service de Physique Théorique, CEA/DSM/SPhT, Unité de recherche associée au CNRS, CEA/Saclay 91191 Gif-sur-Yvette cédex

fbernard@spht.saclay.cea.fr

Abstract These notes present the physics of gravitational lensing in various cosmological contexts. The equations and approximations that are commonly used to describe the displacement field or the amplification effects are presented. Several observational applications are discussed. They range from micro-lensing effects to cosmic shear detection that is a weak lensing effect induced by the large-scale structure of the Universe. The scientific perspectives of this latter application are presented in some details.

Keywords: Cosmology; Lensing; Large-scale structure; Cosmic Shear; Dark matter; Dark energy; Perturbation Theory

1. Introduction

Gravitational lens effects offer a precious mean for probing the matter distribution in the Universe. From the search of matter in the Galactic halo to the study of the large-scale structure of the Universe, gravitational lens surveys represent a unique alternative to galaxy catalogues and have been widely used till now.

The early reports of sound detections of gravitational effects induced by the large-scale structure of the Universe acting on background galaxies date back the beginning of year 2000 [1–4]. These detections have marked the beginning of a new era for the use of lens effects to probe the distribution of matter in the Universe. Unlike galaxy surveys that have been used mainly in the past two decades, cosmic shear surveys directly

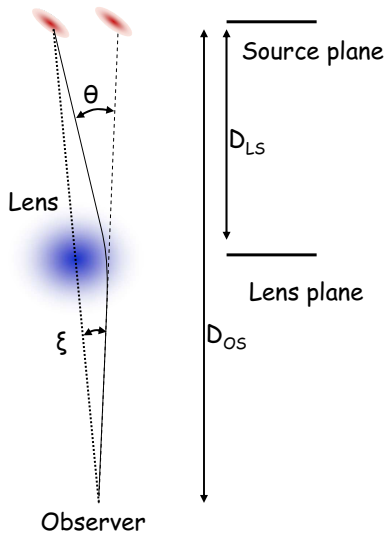

Figure 1.1. The geometrical relationship between the deflection angle θ and the displacement angle ξ.

map the mass, not the light distribution, therefore avoiding the so-called bias problem. Cosmic shear surveys are thus expected to fruitfully complement CMB observations with projects such as CFHTLS and SNAP satellite.

The aim of these lectures is to study the effects of gravitational lenses in those different astrophysical contexts. These notes are voluntarily focused on the fundamental mechanisms and the basic concepts that are useful to describe these effects. A particular emphasis will be put on the subtleties of the scientific exploitation of the cosmic shear surveys.

These notes are organized the following way. In the first section I describe of the basic mechanisms and concepts of gravitational lensing calculations. The computations are illustrated in case of a very simple deflector, a point-like mass distribution. The next section is devoted to aspects of gravitational lenses that are more specific to a cosmological context with an application to galaxy clusters. The remaining sections are devoted to the weak lensing regime and its use is cosmology, the cosmic shear. This is a rapidly developing area that should eventually allow us to map the mass distribution in the Universe. Hints on how this can be used to constrain the cosmological models will be given in the last section.

2. Physical mechanisms

The physical mechanisms of gravitational lenses are well known since the foundation of General Relativity. Any mass concentration is going to deflect photons that are passing by with a fraction angle per unit length, $\delta\theta/\delta s$, given by

$$\frac{\delta\vec{\theta}}{\delta s} = -2\,\vec{\nabla}_x \frac{\phi}{c^2} \tag{1.1}$$

where the spatial derivative is taken in a plane that is orthogonal to the photon trajectory and ϕ is the Newtonian potential [1].

Born approximation and thin lens approximation

In practice, the total deflection angle is at most about an arcmin. This is the case for the most massive galaxy clusters. It implies that in the subsequent calculations it is possible to ignore the bending of the trajectories and calculate the lens effects as if the trajectories were straight lines. *This is the Born approximation.*

Eventually, one can do another approximation by noting that in general the deflection takes place along a very small fraction of the trajectory between the sources and the observer. One can then assume that the lens effect is instantaneous and is produced through the crossing of a plane, the lens plane. *This is the thin lens approximation.*

The induced displacement

The direct consequence of this bending is a displacement of the apparent position of the background objects. This apparent displacement depends on the distance of the source plane, D_{OS}, and on the distance between the lens plane and the source plane D_{LS}. More precisely we have (see Fig. 1.1),

$$\vec{\beta} = \vec{\alpha} - \frac{2}{c^2}\,\frac{D_{LS}}{D_{OS}\,D_{OL}}\,\vec{\nabla}_\alpha \left(\int \mathrm{d}s\ \phi(s,\alpha) \right) \tag{1.2}$$

where $\vec{\alpha}$ is the position in the image plane, $\vec{\beta}$ is the position in the source plane. The gradient is taken here with respect to the angular position (this is why a D_{OL} factor appears). The total deflection is obtained by an integration along the line of sight, assuming the lens is thin. In a cosmological context the exact expressions of the angular distances are not trivial, they depend on the local curvature of the background.

The case of a point-like mass distribution

Multiple images and displacement field. The potential of a point-like mass distribution is given by,

$$\phi(r) = \frac{-G\,M}{r}, \tag{1.3}$$

for an object of mass M. Let me calculate the instantaneous deflection angle at an apparent distance r. We suppose that the impact parameter of the trajectory is r and $\mathbf{x}$ is the abscissa to the point of the trajectory that is the closest to the lens. Along the trajectory the potential is given by,

$$\phi(x) = \frac{-G\,M}{\sqrt{r^2 + x^2}}. \tag{1.4}$$

Then the deflecting angle is given by,

$$\frac{\delta\theta}{\delta x} = -2\,\frac{G\,M\,r}{c^2\,(r^2 + x^2)^{3/2}}. \tag{1.5}$$

The total deflection angle θ is given by the result of the integration of this quantity with respect to x. It gives,

$$\theta = \frac{4\,G\,M}{r\,c^2}. \tag{1.6}$$

It implies that the true position of an object on the sky, β, is related to its apparent position, α, with

$$\vec{\beta} = \vec{\alpha} - \frac{R_E^2}{\alpha^2}\,\vec{\alpha} \tag{1.7}$$

where $\vec{\beta}$ and $\vec{\alpha}$ are 2D angular position vectors (taken from the center of the lens) and R_E is the Einstein radius,

$$R_E = \sqrt{\frac{4\,G\,M}{c^2}\,\frac{D_{LS}}{D_{OS}\,D_{OL}}}. \tag{1.8}$$

One can see that when $\alpha^2 = R_E^2$ the lens and the background objects are necessarily aligned. It implies that, since the optical bench is symmetric around its axis, the observed object appears as a perfect ring. It is worth noting that for this potential, except for this particular position, all background objects have two images. This is however quite specific to a point like mass distribution which has a singular gravitational potential.

The problem is that none of these features are observable when the lens is a star. Let for example assume that we have a one solar mass

star in the halo of our galaxy (therefore at a distance of about 30 *kpc*). The apparent size of such a star is about 10^{-8} arcsec. Its Einstein ring is about 10^{-4} arcsec^2. None of these dimensions are accessible to the observations (the angular resolution of telescope is at best a few tens of arcsec). The Einstein radius is therefore much too small to be actually seen!

Note however that these numbers show that the point-like approximation is entirely justified for a star (the Einstein ring is much more bigger that the apparent size of a star). Simple examination of the scaling in those relations shows that this would not be true for massive astrophysical objects such as galaxies or galaxy clusters.

The detection of gravitational effects due to stars should then be done by another mean: the amplification effect.

The amplification matrix. The case of circular lenses has already given us a clue: when the source is precisely aligned with the lens, the image is no more a point but a circle. One consequence is that the observed total luminosity is much larger than what would have been observed without lenses. The effect is basically due to the variations of the displacement field with respect to the apparent position. These variations induce a change of both the size and shape of the background objects. To quantify this effect one can compute the amplification matrix A which describes the linear transform between the source plane and the image plane,

$$A = \left(\frac{\partial \alpha_i}{\partial \beta_j} \right). \tag{1.9}$$

Its inverse, A^{-1}, is actually directly calculable in terms of the gravitational potential. It is given by the derivatives of the displacement with respect to the apparent position,

$$A^{-1} \equiv \frac{\partial \beta_i}{\partial \alpha_j} = \delta_{ij} - 2 \frac{D_{LS}}{D_{OS}\, D_{OL}} \phi_{,ij}. \tag{1.10}$$

In case of a point-like mass distribution it is easy to see that (coordinates are taken from the center of the lens),

$$A^{-1} = \left(\delta_{ij} \left[1 - \frac{R_E^2}{\alpha^2} \right] + 2 \frac{\alpha_i \alpha_j}{\alpha^4} R_E^2 \right). \tag{1.11}$$

The amplification effect for each image is given by the inverse of the determinant of the amplification matrix computed at the apparent position of the image. The amplification factor is usually noted μ,

$$\mu = 1/\det(A^{-1}). \tag{1.12}$$

In case of the point-like distribution we have (the calculation is simple at the position $\alpha_1 = \alpha,\ \alpha_2 = 0$),

$$\mu = \left| \frac{\alpha^4}{\alpha^4 - R_E^4} \right|, \tag{1.13}$$

for each image. The *total* amplification effect is given by the summation of the two effects for the 2 images,

$$\mu_{\rm tot} = \frac{u^2+2}{u(u^2+4)^{1/2}} \quad \text{with} \quad u = \frac{\beta}{R_E}, \tag{1.14}$$

where β appears to be the impact parameter of the background object in the source plane. The amplification effect is obviously dependent on the impact parameter. If it is changing with time, this effect is detectable. This is the basis of the microlensing experiments : when a compact object of the halo of our galaxy reaches, because of its proper motion, the vicinity of the light path of a background star (from the SMC or the LMC) the impact parameter is changing with time and can be small enough to induce a detectable amplification (when u is about unity, the amplification is about 30%). In practice one observes changes in the magnitude of the remote stars that obey specific properties,

- the time dependence of the amplification is symmetric and has a specific shape;
- the amplification effect is unique;
- the magnitude of the amplification effect is the same in all wavelengths.

The time scale of such an event is about a few days to a few month depending on the mass of the deflectors. Currently a fair number of such events have been recorded and constraints on the content of our halo with low massive compact objects have been put.

3. Gravitational lenses in Cosmology

The extension of the lens equations to a cosmological context raises some technical difficulties because the background in which the objects are embedded is not flat. In particular one must pay attention to the distances that should be employed. The other change is that lenses will now have extended mass distribution.

Cosmological distances and gravitational potential

In cosmology one distinguishes between the radial distance, χ (distance actually travelled on a light cone) and the angular distance D_0 (defined from the apparent size of distant objects). Reminding that

$$\mathrm{d}s^2 = \mathrm{d}t^2 - a^2(t)\left(\frac{\mathrm{d}x^2}{1-kx^2} + x^2\mathrm{d}\theta^2 + x^2\sin^2\theta\mathrm{d}\varphi^2\right) \tag{1.15}$$

The distance χ is directly related to the time dependence of the expansion factor. It is given by,

$$\chi(z) = \int_{t_0}^{t_1}\frac{c\,\mathrm{d}t}{a} = \int_0^{x(z)}\frac{\mathrm{d}x}{\sqrt{1-kx^2}} \tag{1.16}$$

for the distance between $z = 0$ and a plane at redshift z. The distance between two planes at redshifts z_1 and z_2 is simply,

$$\chi(z_2, z_1) \equiv \int_{t_1}^{t_2}\frac{c\,\mathrm{d}t}{a} = \chi(z_2) - \chi(z_1). \tag{1.17}$$

The angular distances can be obtained from the radial ones and are given by,

$$D_0(z) = \frac{1}{\sqrt{-k}}\sinh[\sqrt{-k}\ \chi(z)]. \tag{1.18}$$

and

$$D_0(z_1, z_2) = \frac{1}{\sqrt{-k}}\sinh[\sqrt{-k}\ (\chi(z_2, z_1))], \tag{1.19}$$

where k is the (constant) curvature of the metric (Note that the two distances coincide when $k \to 0$). The exact expressions of these distances as a function on redshifts depend on the time dependence of a and thus on the content of the Universe (and particularly on the vacuum energy density). In case of an Einstein-de Sitter Universe we simply have,

$$D_0(z) = \chi(z) = \frac{c}{H_0}\left(2 - \frac{2}{\sqrt{1+z}}\right). \tag{1.20}$$

In the lens equation the distance to use is the angular distance. This can be unambiguously established by the geometric optic equations.

And the source term of the deflexion is the gravitational potential, ϕ, which in a cosmological context is given by a slightly modified Poisson equation,

$$\Delta_x\phi(\mathbf{x}) = 4\pi\, G\,\overline{\rho}\, a^2\,\delta_{\mathrm{mass}}(\mathbf{x}) \tag{1.21}$$

where δ_{mass} is the local mass density contrast,

$$\delta_{\mathrm{mass}}(\mathbf{x}) = \rho(\mathbf{x})/\overline{\rho} - 1. \tag{1.22}$$

Galaxy clusters as gravitational lenses

The study of galaxy clusters has become a very active field since the discovery of the first gravitational arc in Abell cluster A370 [11]. Galaxy clusters give the most dramatic example of gravitational lens effects in a cosmological context. The difficulty is however to describe the shape of their mass distribution.

The isothermal profile

For an isothermal profile we assume that the local density $\rho(r)$ behaves like,

$$\rho(r) = \rho_0 \left(\frac{r}{r_0}\right)^{-2}. \tag{1.23}$$

With such a density profile the total mass is not finite. So this is not a realistic description but it is a good starting point for the central part of clusters. It is actually more convenient to parameterize the depth of a potential well with the velocity dispersion it induces. Such a dispersion is in principle measurable with the observed galaxy velocity dispersion. It is related to the mass $M(< r)$ included within a radius r,

$$\sigma^2(r) \sim \frac{G\,M(< r)}{r}. \tag{1.24}$$

In case of a isothermal profile, the velocity dispersion is *independent* of the radius and we have

$$\sigma^2 = 2\pi\, G\, \rho_0\, r_0^2. \tag{1.25}$$

The integrated potential along the line-of-sight is given by,

$$\varphi(r) = 2\pi\, \sigma^2\, r. \tag{1.26}$$

As a consequence, the amplitude of the displacement is independent of the distance to the cluster center and

$$\vec{\beta} = \vec{\alpha} - \frac{4\pi}{c^2}\,\frac{D_{LS}}{D_{OS}}\sigma^2\,\frac{\vec{\alpha}}{\alpha}. \tag{1.27}$$

For

$$\alpha = R_E = \frac{4\pi}{c^2}\,\frac{D_{LS}}{D_{OS}}\sigma^2, \tag{1.28}$$

$\alpha^S = 0$ is solution so that R_E corresponds to the radius of a possible "Einstein ring". Note that its size is directly proportional to the square of velocity dispersion (in units of c^2) and to the ratio D_{LS}/D_{OS}. Generically the number of images depends on the value of the impact parameter. If it is smaller that R_E, there are two solutions, otherwise only

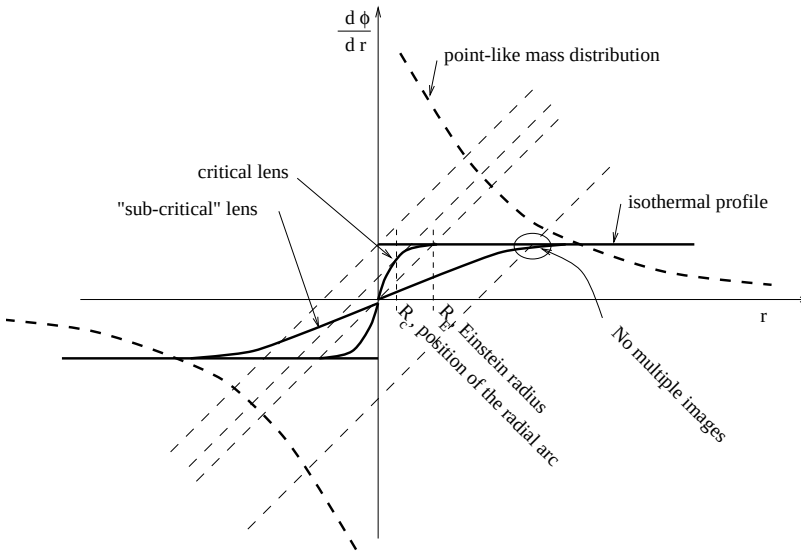

Figure 1.2. Graphical determination of the position and number of images from the shape of the potential.

one. For a galaxy cluster of a typical velocity dispersion of 500 km/s, and for a source plane situated at twice the distance of the lens, the size of the Einstein ring is about 0.5 arcmin that well within observational limits.

Note that the amplification matrix reads,

$$A^{-1} = \begin{pmatrix} 1 & 0 \\ 0 & 1 - \frac{1}{x} \end{pmatrix}, \tag{1.29}$$

where $x = r/R_E$. As a result the amplification factor is given by, $\mu = x/(1-x)$. It becomes infinite when $x \to 1$. It expresses the fact that at the position of the Einstein ring the background objects are infinitely stretched out.

The case of a spherically symmetric mass distribution. Let us consider a more general spherically symmetric profile for the mass distribution. The displacement is then given by,

$$\vec{\beta} = \vec{\alpha}^I - \frac{\mathrm{d}\psi}{\mathrm{d}\alpha}\frac{\vec{\alpha}}{\alpha}, \tag{1.30}$$

where ψ is proportional to the line-of-sight projected potential. It is interesting to visualize this relation with a graphic representation as shown on Fig. 1.2. The number and position of the images of a given background object are given by the number of intersection points between

the curve and a straight line of slope unity. This is a direct consequence of the relation,

$$b - a = -\frac{\mathrm{d}\varphi(a)}{\mathrm{d}a} \tag{1.31}$$

when the potential is computed *along a given axis* that crosses the cluster through the center and b and a are the abscissa on this axis of one given object in respectively the source and the image plane.

In this case the amplification matrix reads,

$$A^{-1} = \begin{pmatrix} 1 - \frac{\partial^2\varphi}{\partial r^2} & 0 \\ 0 & 1 - \frac{1}{r}\frac{\partial\varphi}{\partial r} \end{pmatrix}, \tag{1.32}$$

when it is written in the basis $(\vec{e}_r, \vec{e}_\theta)$. Then the amplification is infinite in two cases, when

$$\frac{\partial^2\varphi}{\partial r^2} = 1 \quad \text{or} \quad \frac{1}{r}\frac{\partial\varphi}{\partial r} = 1. \tag{1.33}$$

The second eigenvalue corresponds to an Einstein ring. The first eigenvalue, however, is associated with an eigenvector that is along the x direction, that is along the radial direction. It can lead to the formation of "radial arc". It graphically corresponds to the case of two merging roots associated to positions close to the origin. That such arcs have been observed gives precious indication on the behavior of the potential near the central part of clusters.

Critical lines and caustics in realistic mass distributions. In realistic reconstructions of lens potential however, it is very rare that the lens has circular shape. Most of the time the mass distribution of the lens is much more complicated. It induces complex features and series of multiple images.

The simplest assumption beyond the spherically symmetric models is to introduce an ellipticity ϵ in the mass distribution,

$$\varphi = \varphi_0\sqrt{1 + r_{\mathrm{em}}^2/r_c^2} \quad \text{with} \quad r_{\mathrm{em}}^2 = \frac{x^2}{(1-\epsilon)^2} + \frac{y^2}{(1+\epsilon)^2}. \tag{1.34}$$

To understand the physics it induces one should introduce the caustics and critical lines. The *critical lines* are the location on the image plane of the points of infinite magnification. The *caustics* are the location of these points on the source plane. These points are determined by the lines on which $\det(A^{-1}) = 0$. For instance the Einstein ring is the critical line for an isothermal profile. Its caustic reduces to one point that can be covered by a background object thus forming a genuine Einstein ring. In general critical lines will be associated with the formation of

arcs produced by background galaxies that happen to be located on the caustics.

In practice the reconstructions of the basic phenomenological effects, position of giant arcs and of multiple images, seen in images of galaxy clusters can be obtained through the superposition of one or very few such elliptical potentials. However the reconstruction of complete galaxy cluster mass maps may eventually requires the use of more complicated models and it can be necessary to perform non-parametric mass reconstructions. A number of important results have been obtained from such observations (see [5] and references therein).

The weak lensing regime

In this section the possibility of using lens effects to probe the large-scale structure of the Universe is considered. The difficulty lies in that the distortion induced by the lenses can be very small. The projected potential should then be reconstructed with a statistical analysis on the deformation effects measured on a lot of background objects. For slightly extended objects such as background galaxies the deformation is described by the amplification matrix, the components of component of which are usually written

$$A^{-1} = \begin{pmatrix} 1-\kappa-\gamma_1 & -\gamma_2 \\ -\gamma_2 & 1-\kappa+\gamma_1 \end{pmatrix}, \tag{1.35}$$

taking advantage of the fact that it is a symmetric matrix. The components of this matrix are expressed in terms of the convergence, κ, (a scalar field) and the shear, γ (a pseudo vector field) with

$$\kappa = \frac{1}{2}\nabla^2\psi; \quad \gamma_1 = \frac{1}{2}(\psi_{,11} - \psi_{,22}) \; ; \quad \gamma_2 = \psi_{,12}, \tag{1.36}$$

with

$$\psi = 2\frac{D_{LS}}{D_{OS}\, D_{OL}}\varphi. \tag{1.37}$$

The convergence describes the linear change of size and the shear describes the deformation. *The weak lensing regime corresponds to small values of κ and γ.*

The consequences of such a transform matrix can be decomposed in two aspects:

- The magnification effect [12, 13]. Lenses induce a change of size of the objects. As the surface brightness is not changed by this effect, the change of surface induces a direct magnification effect

that causes changes in the apparent number density of detected objects. This effect will be ignored in the following.

- The distortion effect. Lenses also induce a change of shape of the background objects. The eigenvalues of the matrix A^{-1} determine the direction and amplitude of such a deformation.

Shapes of background galaxies can then be used to map the distortion field. This is the first step towards the reconstruction of the actual projected mass density of the Universe. The elaboration of methods for reconstructing mass maps from distortion fields is itself not a trivial issue. Following the pioneering work of Kaiser and Squires [14] many methods have been proposed to address this point [15–20] and shown it can be done now with great accuracy.

4. Cosmic Shear: weak lensing as a probe of the large-scale structure

In this section the possibility of using weak lensing analysis for mapping the large-scale structure of the universe is investigated.

Single lens and multiple lenses

At the end of the previous section, it has been stressed that the convergence and shear components all derived from a single scalar field directly proportional to the projected potential. To be more precise if the elements of the amplification matrix are dominated by one single lens then

$$A_{ij}^{-1} = \delta_{ij} - \frac{2}{c^2}\frac{D_{LS}D_{OL}}{D_{OS}}\int_0^{\chi_s} \mathrm{d}\chi' \phi_{,ij}(\chi') \tag{1.38}$$

where $\phi_{,ij}(\chi')$ are the derivatives of the gravitational potential ϕ in comoving coordinates at distance χ' to the observer. The line of sigh integral is done to the source plane distance ${\chi_s}^3$. The expression of the convergence is then particularly interesting. It is obtained from the trace of the expression which makes appear the Laplacian of the potential field, which in turn is proportional to the local density contrast (e.g. Eq. 1.21) so that,

$$\kappa = \frac{3}{2}\Omega_0 \frac{1}{(c/H_0)^2}\frac{D_{LS}D_{OL}}{D_{OS}}\int_0^{\chi_s} \frac{\mathrm{d}\chi'}{a(\chi)}\delta(\chi'). \tag{1.39}$$

Note that the cosmological distances are proportional to c/H_0 so that the κ-δ relation is does not depend on the value of H_0.

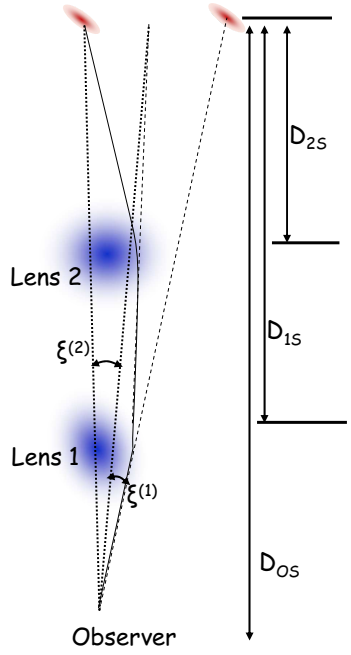

Figure 1.3. The case of a double deflection.

Before further exploration of the phenomenological consequences of this relation, it should be extended to cases where multiple lenses are along the line of sight; a generic situation in a cosmological context.

As on Fig. 1.3 when 2 lenses contribute to the deflexion the total displacement field, ξ, is obtained form the sum of the 2 contribution $\xi^{(1)}$ and $\xi^{(2)}$,

$$\begin{aligned} \xi_i^{\rm tot} &= \xi_i^{(1)} + \xi_i^{(2)} && (1.40)\\ &= -\frac{2}{c^2}\frac{D_{1S}}{D_{OS}D_{O1}}\varphi^{(1)}_{,i} - \frac{2}{c^2}\frac{D_{2S}}{D_{OS}D_{O2}}\varphi^{(2)}_{,i} && (1.41)\end{aligned}$$

where $\varphi^{(n)}_{,i}$ is the gradient of the integrated potential of each lens (assuming each can be approximated by a thin lens). Note however that while the gradient of lens 1 is taken at the image plane position, α^I, the one of lens 2 is taken on the lens 2 plane deformed by the first lens which then read,

$$\alpha_i^{L2} = \alpha_i^I - \frac{2}{c^2}\frac{D_{12}}{D_{O2}\,D_{O1}}\varphi^{(1)}_{,i} \qquad (1.42)$$

As a result the total amplification matrix reads,

$$\begin{aligned}\left(A_{\text{tot.}}^{-1}\right)_{ij} &= \delta_{ij} - \frac{2}{c^2}\frac{D_{1S}}{D_{OS}D_{O1}}\varphi_{,ij}^{(1)} \\ &\quad -\frac{2}{c^2}\frac{D_{2S}}{D_{OS}D_{O2}}\varphi_{,ik}^{(2)}\left(\delta_{kj} - \frac{2}{c^2}\frac{D_{12}}{D_{O2}D_{O1}}\varphi_{,kj}^{(1)}\right) \end{aligned} \quad (1.43)$$

which implies that,

$$A_{\text{tot.}}^{-1} - \text{Id} = A_1^{-1} - \text{Id} + A_2^{-1} - \text{Id} + \frac{D_{12}}{D_{O2}}\frac{D_{OS}}{D_{1S}}\left(A_2^{-1} - Id\right)\left(A_1^{-1} - \text{Id}\right) \quad (1.44)$$

The nontrivial part of the combination effects appear to be quadratic in the convergence and the shear. In the weak lensing regime, by construction we keep only linear terms which implies that

$$A_{\text{tot.}}^{-1} - \text{Id} = \sum_{\text{lenses}}\left(A_i^{-1} - \text{Id}\right). \quad (1.45)$$

The amplification matrix is given by the superposition of lens effects of the different mass layers. Generalizing this result to a continuous field [4], the component of the amplification matrix can then be inferred from the line of sight integration of the gravitational potential angular derivatives,

$$A_{ij}^{-1} = \delta_{ij} - \frac{2}{c^2}\int_0^{\chi_s} \mathrm{d}\chi' \phi_{,ij}\,\frac{D(\chi', \chi_s)}{D(\chi_s)\,D(\chi')} \quad (1.46)$$

In particular the projected convergence reads,

$$\kappa = \frac{3}{2}\Omega_0 \frac{1}{(c/H_0)^2}\int_0^{\chi_s}\frac{\mathrm{d}\chi'}{a(\chi')}\frac{D(\chi', \chi_s)\,D(\chi')}{D(\chi_s)}\,\delta_{\text{mass}}(\chi') \quad (1.47)$$

Basics of phenomenology

The previous relation basically tells us that

$$\kappa = \int \mathrm{d}\chi\, w(\chi)\,\delta_{\text{mass}} \quad (1.48)$$

where $w(\chi)$ is a line-of-sight weight function proportional to Ω_0.

From the previous equation it can be readily noted that the amplitude of the convergence field is expected to be both proportional to Ω_0 and to the amplitude of the 3D mass density fluctuation. Extra dependence with the other cosmological parameters (Ω_0, Ω_Λ) can take place through

the growth rate of the fluctuation and the cosmological distances if the source plane is at large enough redshift (comparable to unity).

To a very crude approximation we then have

$$\sigma_\kappa \sim \Omega_0 \sigma_8 \tag{1.49}$$

where σ_8 is the amplitude of the matter density fluctuations at $8h^{-1}$Mpc scale.

In the following we will try to examine in more details the κ-δ relation.

Convergence and shear correlation functions and power spectra

It can be easily shown that

$$\partial_1\kappa = \partial_1\gamma_1 + \partial_2\gamma_2 \tag{1.50}$$
$$\partial_2\kappa = -\partial_2\gamma_1 + \partial_1\gamma_2. \tag{1.51}$$

and which also gives,

$$\Delta\kappa = \left(\partial_1^2 - \partial_2^2\right)\gamma_1 + 2\partial_1\partial_2\ \gamma_2 \tag{1.52}$$

These real space relations can be transformed into Fourier space relations. The Fourier modes of the convergence field is defined as

$$\kappa(\mathbf{x}) = \int \frac{\mathrm{d}^2\mathbf{l}}{2\pi}\,\kappa(\mathbf{l})\,\exp(\mathrm{i}\mathbf{l}.\mathbf{x}) \tag{1.53}$$

where the survey is assumed to be small enough so that the decomposition can be made into plane waves[5]. The above relations imply that

$$\gamma_1(\mathbf{l}) = \frac{l_1^2 - l_2^2}{l^2}\kappa(\mathbf{l}) \tag{1.54}$$
$$\gamma_2(\mathbf{l}) = \frac{2l_1\,l_2}{l^2}\kappa(\mathbf{l}). \tag{1.55}$$

According to our current cosmological principles, any angular survey is expected to be statistically isotropic so that ensemble averages of product of 2 Fourier modes $\kappa(\mathbf{l})$ are expected to behave like,

$$\langle\kappa(\mathbf{l})\kappa(\mathbf{l}')\rangle = \delta_{\mathrm{Dirac}}(\mathbf{l}+\mathbf{l}')\,P_\kappa(l) \tag{1.56}$$

and then the 2-point correlation function of the field κ is

$$\langle\kappa(\mathbf{x})\kappa(\mathbf{x}')\rangle = \int \frac{\mathrm{d}^2\mathbf{l}}{(2\pi)^2}\,P_\kappa(l)\exp[\mathrm{i}\mathbf{l}.(\mathbf{x}-\mathbf{x}')]. \tag{1.57}$$

And from (1.54) it is not too difficult to show that,

$$\langle\kappa(\mathbf{x})\kappa(\mathbf{x}')\rangle = \langle\gamma_1(\mathbf{x})\gamma_1(\mathbf{x}')\rangle + \langle\gamma_2(\mathbf{x})\gamma_2(\mathbf{x}')\rangle; \quad (1.58)$$

$$\langle\gamma_1(\mathbf{x})\gamma_2(\mathbf{x}')\rangle = 0 \quad (1.59)$$

The convergence power spectrum in the small angle approximation

The aim of this paragraph is to explicit the relation between the convergence power spectrum and the 3D matter power spectrum. To do that we will explicit the computation of the 2-point correlation of the convergence power spectrum. The 2-point κ correlation function reads,

$$\langle\kappa(\mathbf{x})\kappa(\mathbf{x}')\rangle = \int \mathrm{d}\chi\mathrm{d}\chi'\, w(\chi)\, w(\chi')\, \langle\delta(\chi, D\mathbf{x})\delta(\chi', D'\mathbf{x}')\rangle \quad (1.60)$$

which makes intervene the 2-point matter correlation function between points at radial distance respectively χ and χ' and at angular distance $D\mathbf{x}$ and $D'\mathbf{x}'$. This expression can be written in terms of the 3D matter density power spectrum P_δ,

$$\langle\kappa(\mathbf{x})\kappa(\mathbf{x}')\rangle = \int \mathrm{d}\chi\mathrm{d}\chi'\, w(\chi)\, w(\chi') \int \frac{\mathrm{d}^3\mathbf{k}}{(2\pi)^3}\, P_\delta(k)\, \exp[\mathrm{i}\, k_r(\chi-\chi') + \mathrm{i}\mathbf{k}_\perp.(D\mathbf{x} - D'\mathbf{x}')] \quad (1.61)$$

where the wave vector $\mathbf{k}$ has been decomposed into its radial component k_r and its tangential components $\mathbf{k}_\perp$. Unless the very long wave fluctuations dominate the matter power spectrum, the typical values for k_r and $k_\perp$ that will dominate this integral are about respectively 1/Depth and $1/(|\mathbf{x}-\mathbf{x}'|\text{Depth})$ where Depth is the depth of the survey. In the small angle approximation it means that $k_r \ll k_\perp$. The integral over k_r can be done explicitly and it leads to $\delta_{\text{Dirac}}(\chi-\chi')$. As a result, we have

$$\langle\kappa(\mathbf{x})\kappa(\mathbf{x}')\rangle = \int \mathrm{d}\chi\, w^2(\chi) \int \frac{\mathrm{d}^2\mathbf{k}}{(2\pi)^2}\, P_\delta(k)\, \exp[\mathrm{i}D\mathbf{k}.(\mathbf{x}-\mathbf{x}')] \quad (1.62)$$

which can be rewritten as,

$$\langle\kappa(\mathbf{x})\kappa(\mathbf{x}')\rangle = \int \frac{\mathrm{d}^2\mathbf{k}}{(2\pi)^2}\, \exp[\mathrm{i}\mathbf{l}.(\mathbf{x}-\mathbf{x}')] \int \mathrm{d}\chi\, \frac{w^2(\chi)}{D^2}\, P_\delta\left(\frac{l}{D}\right). \quad (1.63)$$

By identification we obtain the expression of the convergence power spectrum

$$P_\kappa(l) = \int \mathrm{d}\chi\, \frac{w^2(\chi)}{D^2}\, P_\delta\left(\frac{l}{D}\right). \quad (1.64)$$

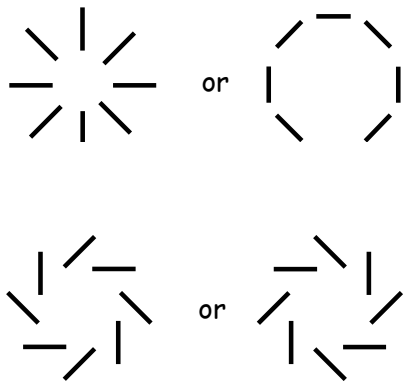

Figure 1.4. Shear configuration for pure E modes (top) and pure B modes (bottom).

It is therefore possible to relate the amplitude of the convergence field to the amplitude and shape of the matter fluctuations. The result can be expressed the r.m.s. of the convergence fluctuation in a disc of radius θ_0,

$$\sigma_\kappa \approx 0.01 \left(\frac{\theta_0}{1\,\mathrm{deg}}\right)^{-(n+2)/2} \sigma_8\, \Omega_0^{0.8}\, z_s^{0.75} \tag{1.65}$$

where σ_8 is the rms of the matter density fluctuations at $8\,h^{-1}$Mpc scale and n is the power spectrum index.

The question now is whether it is observable or not. This signal has to be above the systematics (that depends on what you use to do the measurements) and above the (white) noise due to the intrinsic shape fluctuations of the source galaxies. In practice the measurement is made in the following way. Galaxy ellipticity,25000 ϵ, are measured and a "super" pixel (say of the order of a few arcmin size) and averaged out. In the weak lensing regime we have,

$$\epsilon^I = \epsilon^S + \gamma \tag{1.66}$$

so that the average ellipticity in the image plane reduces to the shear value if, as expected, the average ellipticity is zero in the source plane.

One important practical question is then the level of systematics. It is possible to do a diagnosis of it by taking advantage of the geometrical properties of the shear field, e.g. the fact that it is a potential field.

The E and B fields

As was stressed before, what is observed is the shear field. In practice it is likely that the measured shear field is not purely of cosmological origin due to contamination or systematics effects. The geometrical

properties of the cosmological shear field can however be used to derive means for testing the amount of systematics in the data. The idea is the following. Any 2D spin 2 vector field can be decomposed into a scalar and a pseudo scalar parts. They are defined through their Laplacian,

$$\Delta E = (\partial_1^2 - \partial_2^2)\gamma_1 + 2\partial_1\partial_2\gamma_2 \quad (1.67)$$
$$\Delta B = -2\partial_1\partial_2\gamma_1 + (\partial_1^2 - \partial_2^2)\gamma_2 \quad (1.68)$$

In case the components γ are truly those of a cosmological shear field there would be no B components and E identifies with κ. E is a scalar field: it is invariant under parity change. B is a pseudo scalar field: it changes sign under parity change. These properties can be appreciated on Fig. 1.4 where shear configuration for respectively E and B modes are presented. The E-mode shear field configurations are unaffected by parity changes; the ones for the B modes are changed (in one-another).

The decomposition in E and B components is however not trivial because the relation between E and B and the shear field is non local. It is however possible to have a quasi-localized relation if one considers those field when they are filtered with a compensated filter - that is a filter with 0 integral that therefore smoothes out the long wavelength modes [6]. Let me denote $\hat{E}$ and $\hat{B}$ such quantities in the following. Then formally $\hat{E}$ (at the origin) can be written as

$$\hat{E} = \int \mathrm{d}^2\mathbf{x}'\, E(\mathbf{x}')\; W_c(\mathbf{x}') \quad (1.69)$$

where W_c is a compensated filter. Because it is a compensated filter its Fourier transform can be written $k^2\tilde{W}(k)$ so that

$$\hat{E} = \int \mathrm{d}^2\mathbf{x}'\, \Delta E(\mathbf{x}')\; \tilde{W}(x') \quad (1.70)$$

where $\tilde{W}(x')$ is the real-space Fourier transform of $\tilde{W}(k)$. Then

$$\hat{E} = \int \mathrm{d}^2\mathbf{x}'\, \left[(\partial_1^2 - \partial_2^2)\gamma_1(\mathbf{x}') + 2\partial_1\partial_2\gamma_2(\mathbf{x}')\right] \tilde{W}(x') \quad (1.71)$$

which after integration by parts can be written

$$\hat{E} = \int \mathrm{d}^2\mathbf{x}'\, \begin{pmatrix} \cos(2\theta') \\ \sin(2\theta') \end{pmatrix} . \begin{pmatrix} \gamma_1 \\ \gamma_2 \end{pmatrix} \left(\tilde{W}''(x') - \frac{\tilde{W}'}{x'}(x')\right). \quad (1.72)$$

where θ' is the angle of $\mathbf{x}'$. What we obtain here is an integral of the radial component of γ on an area with a given profile $p(x')$, e.g.

$$\hat{E} = \int \mathrm{d}r\; p(r) \int \mathrm{d}\theta\; \gamma_r(\theta). \quad (1.73)$$

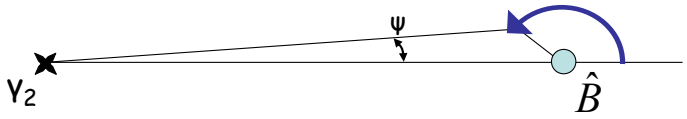

Figure 1.5. Sketch of the integration path for Eq. 1.74

Similarly $\hat{B}$ corresponds to an integral of tangential component of the shear,

$$\hat{B} = \int \mathrm{d}r\ p(r) \int \mathrm{d}\theta\ \gamma_T(\theta). \tag{1.74}$$

Consistency relations for the shear correlation functions.

The observational data allow the estimation of two different correlation functions at finite distance. The one between the radial components, $\xi_{++}(x)$ and the one between the transverse component $\xi_{\times\times}(x)$ (the cross-correlation between the components being 0 for symmetry reasons).

However in the absence of B field, these two functions should be related together, e.g. they all come from a single power spectrum. Although it is possible to obtain a functional relation from a direct approach, I present here a way to get such a relation from simple physical considerations. Indeed a vanishing B implies that both $\langle\gamma_1(\mathbf{x}_1)\hat{B}(\mathbf{x}_2)\rangle$ and $\langle\gamma_2(\mathbf{x}_1)\hat{B}(\mathbf{x}_2)\rangle$ are zero. This is true for parity reasons for the first one if $\mathbf{x}_2 - \mathbf{x}_1$ is on the horizontal axis. Imposing that the second one vanishes will lead to a non trivial relation between ξ_{++} and $\xi_{\times\times}$.

From the expression of $\hat{B}$ we have

$$\begin{aligned}\langle\gamma_2(\mathbf{x}_1)\hat{B}(\mathbf{x}_2)\rangle &= \int \mathrm{d}r\, p(r) \int_0^{2\pi} \mathrm{d}\theta\, (-\sin(2\theta)\langle\gamma_2(\mathbf{x}_1)\gamma_1(\mathbf{x}')\rangle + \\ &\qquad \cos(2\theta)\langle\gamma_2(\mathbf{x}_1)\gamma_2(\mathbf{x}')\rangle)\end{aligned} \tag{1.75}$$

where $\mathbf{x}'$ is $\mathbf{x}' = \mathbf{x}_2 + r(\cos\theta, \sin\theta)$. The correlations $\langle\gamma_2(\mathbf{x}_1)\gamma_1(\mathbf{x}')\rangle$ and $\langle\gamma_2(\mathbf{x}_1)\gamma_2(\mathbf{x}')\rangle$ can be expressed in terms of ξ_{++} and $\xi_{\times\times}$,

$$\langle\gamma_2(\mathbf{x}_1)\gamma_1(\mathbf{x}')\rangle = \sin(2\psi)\cos(2\psi)[\xi_{++}(x') - \xi_{\times\times}(x')] \tag{1.76}$$

$$\langle\gamma_2(\mathbf{x}_1)\gamma_2(\mathbf{x}')\rangle = \sin^2(2\pi)\xi_{++}(x') + \cos^2(2\psi)\xi_{\times\times}(x') \tag{1.77}$$

where ψ is defined on Fig. 1.5 and $x' = |\mathbf{x}' - \mathbf{x}_1|$. The above integral should vanish for any function $p(r)$, therefore in particular when the

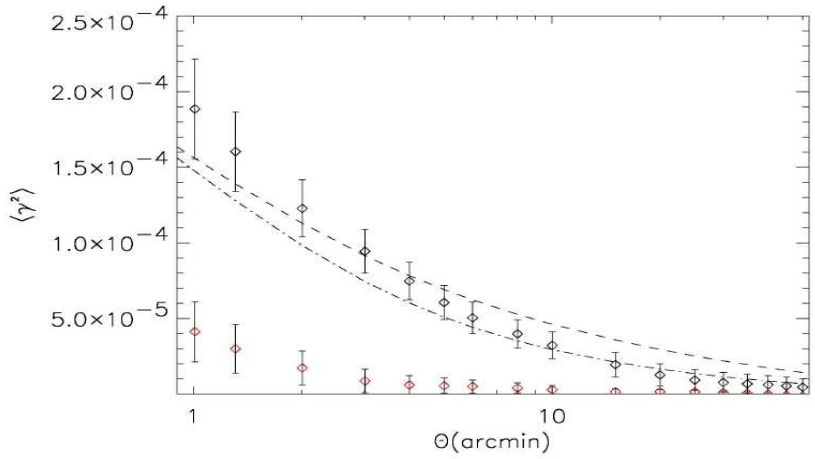

Figure 1.6. Measured behavior of the E (upper black diamonds) and B (lower red diamonds) mode components in the DESCART cosmic shear surveys (van Waerbeke, private communication).

contributing values of r are much smaller than $|\mathbf{x}_2 - \mathbf{x}_1|$. It is then possible to expand all quantities with respect to r (up to second order):

$$\begin{aligned} x' &= x + r\,\cos\theta + \frac{r^2}{2x^2}\sin^2\theta + \dots \\ \xi(x') &= \xi(x) + r\cos\theta\;\xi'(x) + \frac{r^2}{2x}\sin^2\theta\;\xi'(x) + \frac{r^2}{2}\cos^2\theta\;\xi''(x) + \dots \\ \sin\psi &= \frac{r}{x}\sin\theta - \frac{r^2}{x^2}\sin\theta\cos\theta + \dots \end{aligned}$$

After integration over θ we have,

$$\xi''_{\times\times} + 3\frac{\xi'_{\times\times}}{x} + 4\frac{\xi_{\times\times}}{x^2} - 4\frac{\xi'_{++}}{x} - 4\frac{\xi_{++}}{x^2} = 0 \tag{1.78}$$

($\int_0^{2\pi} \mathrm{d}\theta\cos(2\theta)\sin^2\theta = -(2\pi)/4$, $\int_0^{2\pi} \mathrm{d}\theta\cos(2\theta)\cos^2\theta = (2\pi)/4$). This expression can be written in an integral form. It allows to make important consistency checks in the data samples.

On Fig. 1.6 is presented what can be actually observed in data sets. B modes are shown to be detectable at very small angular scale. This could be due to the fact that close pairs may actually have gone through a physical interaction. At large scale however the B modes are found to be negligible, opening the way to a far reaching use of such catalogues.

The resulting dark matter power spectrum is shown on Fig. 1.7 where results from weak lensing surveys are checked against CMB observations.

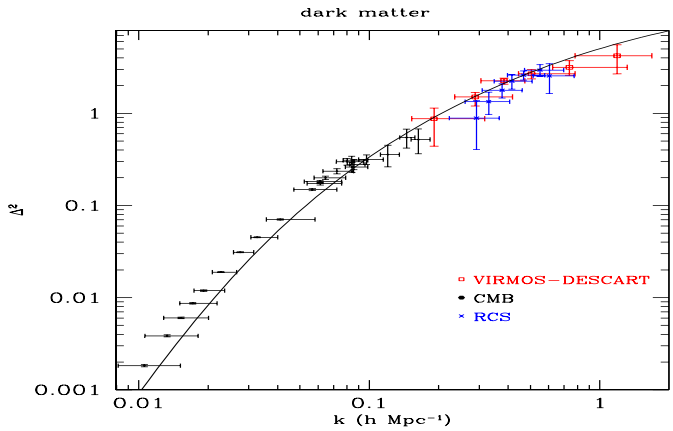

Figure 1.7. Shape of the dark matter power spectrum as reconstructed from weak lensing data (red squares, Virmos-Descart survey). It is confronted to what is expected from CMB anisotropy power spectrum (small black squares).

5. Conclusions and perspectives: cosmic shear in a precision cosmology era

Because cosmic shear surveys probe the dark matter distribution up to significant redshift, it is a probe of the details of the gravitational dynamics. With large scale surveys it then becomes possible to test the details of large-scale structure growth with unprecedented accuracy.

It is possible for instance to test the mode couplings as the gravitational instabilities develop. The amount of non-Gaussianities embedded in cosmic shear surveys then betrays the details of the gravitational instability scenario, allowing for instance the possibility of measuring the mass density of the universe in a totally independent way. That would contribute in the consolidation of the current concordance model of cosmology.

Actually the crucial issue raised by this model is the dark energy, a putative energy density associated with the cosmological vacuum, whose existence is strongly suggested from the current cosmological observations. This is a major issue from a theoretical physics point of view. At this moment it is not clear that its solution lies in a change of the gravity law at very large scale (as could the existence of extra spatial dimension imply) or to the existence of a new form of matter in the universe. In all cases it is to be stressed that it is essentially a low redshift phenomenon that cosmic shear observations should allow to address. In such surveys

precise quantitative tests can be designed where the very details of the model of the structure growth can be scrutinized[36].

Notes

1. We will see in section 1.3 what is its meaning in a cosmological context.
2. To do this calculation it is useful to know that the horizon of a one solar mass black hole, $r = 2\,G\,M_\odot/c^2$, is about 3 km.
3. Note that the source plane is not necessarily thin. The result is then obtained by a convolution of this expression by the source plane profile. It does not change the discussions presented here so that it will be ignored in the following.
4. A rigorous derivation of these formulae can be found in Sachs [10] where the equations of the geometric optics applied to a light bundle are derived in the context of a weakly perturbed FRW metric.
5. If not, the convergence field has to be decomposed into spherical harmonics and the shear components into mathematical extensions of those.
6. When filtered in such a way the convergence field is called the *mass aperture*.

References

[1] Van Waerbeke, L., Mellier, Y., Erben, T., Cuillandre, J.C., Bernardeau, F., Maoli, R., Bertin, E., Mc Cracken, H., Le Fèvre, O., Fort, B., Dantel-Fort, M., Jain, B., Schneider, P., 2000, A& A, 358, 30

[2] Kaiser, N., Wilson, G., Luppino, G.A., 2000, astro-ph/0003338

[3] Bacon, D., Refregier, A., Ellis, R., 2000 *Mon. Not. R. astr. Soc.* **318**, 625

[4] Wittman, D.M., Tyson, J.A., Kirkman, D., Dell'Antonio, I., Bernstein, G., 2000, Nature, 405, 143

[5] Mellier, Y. 1999, *Annual Review of Astr. & Astrophys.* **37**, 127

[6] Misner, C.W. Thorne, K. & Wheeler, J.A. 1973, Gravitation, San Francisco, Freeman.

[7] Peebles, P.J.E. 1980; The Large–Scale Structure of the Universe; Princeton University Press, Princeton, N.J., USA;

[8] Schneider, P., Ehlers, J., Falco, E. E. 1992, *Gravitational Lenses*, Springer.

[9] Bernardeau, F., 1998, in "Theoretical and Observational Cosmology", proc. of Cargèse summer school, August 17-29 1998, ed. M. Lachièze-Rey

[10] Sachs, R. K. 1961, *Proc. Roc. Soc. London* A**264**, 309

[11] Soucail, G., Mellier, Y., Fort, B., Mathez, G. & Cailloux, M., *Astr. & Astrophys.* in press191L191988

[12] Broadhurst, T. astro-ph/9511150.

[13] Broadhurst, T., Taylor, A.N., Peacock, J. 1995 *Astrophys. J.* **438**, 49

[14] Kaiser, N. & Squires, G. 1993 *Astrophys. J.* **404**, 441

[15] Kaiser, N. 1992 *Astrophys. J.* **388**, L72

[16] Kaiser, N. 1995 *Astrophys. J.* **439**, 1

[17] Bartelmann, M., Narayan, R., Seitz, S. & Schneider, P., 1996, *Astrophys. J.* **464**, 115

[18] Seitz, C., Schneider, P., 1995 *Astr. & Astrophys.* **297**, 247

[19] Seitz, S., Schneider, P., 1996 *Astr. & Astrophys.* **305**, 388

[20] Seitz, S., Schneider, P., Bartelmann, M., 1998 *Astr. & Astrophys.* **337**, 325S

[21] Bertschinger, E. 1996, in "Cosmology and Large Scale Structure", Les Houches Session LX, August 1993, NATO series, eds. R. Schaeffer, J. Silk, M. Spiro, J. Zinn-Justin, Elsevier Science Press

[22] Bernardeau, F., van Waerbeke, L. & Mellier, Y. 1997, *Astr. & Astrophys.* **324**, 15

[23] Villumsen, J. V. 1996, *Mon. Not. R. astr. Soc.* **281**, 369

[24] Miralda-Escudé, J. 1991 *Astrophys. J.* **380**, 1

[25] Jain, B., Seljak, U. 1997, *Astrophys. J.* **484**, 560

[26] Blandford, R. D., Saust, A. B., Brainerd, T. G., Villumsen, J. V. 1991, *Mon. Not. R. astr. Soc.* **251**, 600

[27] Kaiser, N., Squires, G. & Broadhurst, T. 1995 *Astrophys. J.* **449**, 460

[28] A.J.S. Hamilton, P. Kumar, E. Lu, and A. Matthews, 1991 *Astrophys. J. Letter* **374**, L1

[29] J. A. Peacock and S. J. Dodds, 1996 *Mon. Not. R. astr. Soc.* **280**, L19

[30] J. A. Peacock and S. J. Dodds, 1994 *Mon. Not. R. astr. Soc.* **267**, 1020

[31] K. Benabed, F. Bernardeau, 2001 *Phys. Rev. D* **64**, 083501

[32] Ph. Brax, J. Martin, 2000 *Phys. Rev. D* **61**, 103502

[33] Ph. Brax, J. Martin, 1999 *Physics Letter B* **468**, 40

[34] see the CFHLS web site, http://www.cfht.hawaii.edu/Science/CFHLS/

[35] F. Bernardeau, S. Colombi, E. Gaztañaga, R. Scoccimaro, 2002 *Physics Reports* **367**, 1

[36] F. Bernardeau, 2003, Rep. Prog. Phys., 66, 691-736

[37] L. Hui, 1999 *Astrophys. J. Letter* **519**, L9